Influence of Implant Number on Peri-Implant and Posterior Edentulous Area Strains in Mandibular Overdentures Retained by the New Ti–Zr (Roxolid®) Mini-Implants as Single-Units: In Vitro Study

Puljić, Dario; Čelebić, Asja; Kovačić, Ines; Petričević, Nikola

Source / Izvornik: **Applied Sciences, 2024, 14**

Journal article, Published version
Rad u časopisu, Objavljena verzija rada (izdavačev PDF)

https://doi.org/10.3390/app14052150

Permanent link / Trajna poveznica: https://urn.nsk.hr/urn:nbn:hr:127:958952

applied sciences

MDPI

Article

Influence of Implant Number on Peri-Implant and Posterior Edentulous Area Strains in Mandibular Overdentures Retained by the New Ti–Zr (Roxolid®) Mini-Implants as Single-Units: In Vitro Study

Dario Puljic *, Asja Celebic *, Ines Kovacic and Nikola Petricevic

Department of Removable Prosthodontics, University of Zagreb School of Dental Medicine, 10000 Zagreb, Croatia; kovacic@sfzg.hr (I.K.); petricevic@sfzg.hr (N.P.)
* Correspondence: dpuljic@sfzg.hr (D.P.); celebic@sfzg.hr (A.C.)

Abstract: The new Ti–Zr (Roxolid®) mini-implants have not yet been fully researched. We analyzed peri-implant and posterior edentulous area microstrains during mandibular overdenture (OD) loading at different sites with different extents of forces when one-, two-, three-, or four- mini dental implants (MDIs) as single-units supported the respective ODs. The models were designed from cone beam computed tomography (CBCT) scans of an appropriate patient with narrow ridges. The mucosal thickness was 2 mm. Strain gauges were bonded on the vestibular and oral peri-implant sites, and in the distal edentulous area under the saddles. The loads were applied posteriorly bilaterally and unilaterally with 50, 100 and 150 N forces, and anteriorly with 50 and 100 N forces. Each loading was repeated 15 times. Statistical analysis included descriptive statistics, boxplots and the MANOVA. Higher forces induced higher peri-implant microstrains, as well as unilateral loadings, especially on the loaded side, in all models except the one-MDI model where anterior loads (100 N) elicited the highest peri-implant microstrain (1719.35 ± 76.0). The highest microstrains during unilateral posterior loading (right side) with 150 N force were registered from the right MDI in the two-MDI model (1836.64 ± 63.0). High microstrains were also recorded on the left side (1444.48 ± 54.6). By increasing the number of implants, peri-implant microstrains and those in the edentulous area decreased. In the three- and four-MDI models, higher microstrains were found in the posterior than in the anterior MDIs under posterior loadings. None of the recorded microstrains exceeded bone reparatory mechanisms, although precaution and additional research should be provided when only one or two MDIs support ODs.

Keywords: Ti–Zr mini-implants; single units; strain gauges; mandibular overdenture; different number of mini-implants; loading forces; loading position; dentistry; oral surgery

Citation: Puljic, D.; Celebic, A.; Kovacic, I.; Petricevic, N. Influence of Implant Number on Peri-Implant and Posterior Edentulous Area Strains in Mandibular Overdentures Retained by the New Ti–Zr (Roxolid®) Mini-Implants as Single-Units: In Vitro Study. *Appl. Sci.* **2024**, *14*, 2150. https://doi.org/10.3390/app14052150

Academic Editor: Andrea Scribante

Received: 28 January 2024
Revised: 1 March 2024
Accepted: 2 March 2024
Published: 4 March 2024

1. Introduction

In completely edentulous patients with a reduced alveolar ridge width, the insertion of four mini-dental implants (MDI) for mandibular overdenture (OD) retention and support is the alternative option to the insertion of two standard-sized implants [1–11]. Bone augmentation can be avoided by the insertion of narrow implants, which shortens the duration of treatment, providing a less traumatic surgical protocol [1–5]. Narrow dental implants (NDIs) are divided into three categories depending on their diameters: Category 3 (>3.3 mm–3.5 mm wide), Category 2 (>2.5 mm–<3.3 mm), and Category 1 (≤2.5 mm wide) [12]. The one-piece mini-implants are listed in category 1, i.e., the narrowest NDI category (diameter ≤ 2.5 mm) [12]. Narrow implants are usually made of Ti90Al6V4 alloy, which has better mechanical properties than pure titanium. The insertion of four MDIs made of Ti90Al6V4 alloy in the mandible has been approved as a successful treatment option for the retention of a mandibular OD in many prospective clinical studies [1–10,13–15].

Even the insertion of only three MDIs in the mandible for complete OD retention showed very good outcomes in a five-year clinical study [15]. Insertion of two MDIs showed good survival rates and low amounts of marginal bone loss only when used for retention of removable partial dentures [16–18]. However, the clinical outcomes of only two MDIs retaining a complete mandibular OD are still doubtful [19–22]. To the best of our knowledge, no longitudinal clinical reports are available when only one MDI, inserted in the midline of the mandible, was used for the retention of a complete OD.

In 2009, the Ti85Zr15 alloy (Roxolid®) was introduced by the company Straumann Group. It showed very good mechanical properties and excellent osseointegration. Moreover, in many clinical prospective studies, narrow-diameter implants in categories 3 and 2 had very good performance when they supported fixed partial dentures [23–25]. Recently, in 2019, the new mini-implant system (category 1 of narrow implants, 2.4 mm wide) made of the Roxolid® (Ti–Zr) alloy (Straumann® Mini Implant System) was released on the dental market. Innovation of the new Ti–Zr MDIs included the new retention system (Straumann® Optiloc® Retentive System, i.e., prosthetic connection coated with an amorphous diamond-like carbon surface (ADLC) and a female PEEK matrix insert incorporated into titanium housing. The new mini-implant Ti–Zr system allows a choice of appropriate transmucosal heights. Four Roxolid® MDIs have been proposed for the retention of a mandibular OD, and six for the retention of a maxillary OD. Outcomes of four Roxolid® alloy MDIs retaining a mandibular OD in a prospective clinical study are available only for one year of their clinical use but with excellent results [26]. Due to the very good mechanical properties of the new Ti–Zr mini-implant system and the excellent osseointegration of the alloy, it would be interesting to find out whether less than the recommended four Ti–Zr mini-implants inserted in the mandible as single-units can successfully support a mandibular OD. In vitro studies are required before the safe clinical utilization of any new material, clinical technique or modification of any procedures [27–29]. Due to the difference in the stiffness of the implant material and the bone, the highest stress is distributed at the implant–bone interface. Peri-implant strains below 3000 microstrains represent the criterion for the long-term survival of any implant supporting a denture [27]. A model mimicking the "in vivo" situation and measuring peri-implant strains is beneficial to providing insights into the real clinical situation.

Therefore, this "in vitro" study was designed to analyze microstrains around Ti–Zr mini-implants as well as microstrains in the posterior edentulous area when different numbers of single-unit MDIs were inserted. The respective ODs were loaded at different sites and with different loading forces.

2. Materials and Methods

2.1. Mandibular Models

All experiments were performed on models of the same mandible. CBCT (ProMax 3D, Planmeca, Helsinki, Finland) scans of a completely edentulous patient with a narrow residual ridge were chosen. A virtual model was created using the Amira software (Amira, v4.1, Zuse Institute Berlin; Visage Imaging GmbH, Berlin, Germany). Mini-implant positions were planned using the Blender® software (Blender®, v2.79b, Amsterdam, The Netherlands). Four models were designed: one model with four holes for the insertion of four MDIs (in positions of previous first premolars and second incisors on the right and left sides of the mandible). Another model had three holes for the insertion of three MDIs (two posterior MDIs in the positions of previous distoproximal surfaces of the right and left canines, and one anterior MDI in the midline of the mandible). One model had two holes for the insertion of two MDIs (in positions of the previous left and right mandibular canines). The fourth model was designed with only one hole in the midline for the insertion of only one MDI. The length of the holes was 10 mm (equal to the length of the MDIs), while the width of the holes was 2.3 mm, i.e., 0.1 mm narrower than the implant body diameter (2.4 mm). The narrower diameter of the holes was to ensure the stability of implants in the models.

Stereolithographic 3D printing technology (Form 2, Formlabs, Somerville, MA, USA) and Gray photopolymer resin (GRAY FLGPGR04; Formlabs, Somerville, MA, USA) were used for all models. After printing, further processing included immersing the model in 95% isopropyl alcohol (IPA) (Izopropil alkohol, Medimon d.o.o., Split, Croatia) for one minute and then additionally for 15 min in a new container of IPA to rinse the residual resin. After cleaning, a 30-min polymerization with the 36 W UV-A halogen lights (Dentsply Sirona Heliodent Plus, Display Sirona, York, PA, USA) and 30-min heating in a chamber at 60 °C were performed. All models of the mandible were made of the same material, which is, according to its mechanical properties, similar to the D2 bone.

2.2. Implant Insertion and Artificial Mucosa

For each mandibular model, an artificial mucosa was made from vinyl-polysiloxane impression material (3M™ Express™ XT Light Body Quick, Seefeld, Germany) of uniform thickness (2 mm). To ensure uniform thickness, the molds into which the impression material was injected were designed virtually (Amira v4.1, Zuse Institute Berlin; Visage Imaging GmbH, Berlin, Germany) for the 2.0 mm thick mucosa with one, two, three or four perforations at sites where the MDI insertions were planned. The molds were 3D-printed. Impression material (a-silicone) was injected into each mold, and after setting, the artificial mucosa was transferred to the respective model of the mandible, depending on the number of holes.

In each hole (2.3 mm wide), an MDI with a diameter of 2.4 mm and a length of 10 mm (Straumann® Mini Implant, Institute Straumann AG, Basel, Switzerland) was inserted. The gingival MDI height of 2.8 mm (i.e., the height of the polished neck of the implant) was chosen from the Straumann® Mini Implants. Mini-implants were inserted using the torque wrench BLX Torque Control Device (Institute Straumann AG, Basel, Switzerland). The insertion torque (measured using a torque wrench during insertion) varied for a very small amount among MDIs (from 36 to 43 Ncm). The torque values recommended by the manufacturer for immediate loading are $\geq$35 Ncm.

2.3. Overdenture Fabrication

After MDI insertion, the models were scanned (3Shape 3E, 3Shape, Copenhagen, Denmark, 2020) to design the respective ODs. The design of the metal framework for the dentures was generated using computer-aided design (CAD) technology in the 3Shape software (3Shape, v.20.1, Copenhagen, Denmark). Four metal skeletons were created. Printed metal frameworks were manufactured by Wironium® RP metal powder (BEGO, Bremen, Germany) using Sisma Mysint100 Dual laser (Sisma, Piovene Rocchette, Italy). After metal frameworks were finished, artificial teeth were set up (Cross-linked, Polident, Nova Gorica, Slovenia) in a wax rim. Denture processing and acrylic resin polymerization were conducted according to the manufacturer's recommendation (Ivoclar ProBase Hot Denture Resin, Ivoclar Vivadent, Schaan, Liechtenstein). Finally, the ODs were polished. Metal housings for the Optiloc® (Institute Straumann AG, Basel, Switzerland) retention matrices with the medium (yellow) retention inserts (1200 g of the retention force each) were built in the overdenture simultaneously with the overdenture polymerization.

2.4. Strain Gauge Bonding

To measure peri-implant and posterior edentulous area microstrains, strain gauges (SG) (KFGS-1N-120-C1-11N30C2, Kyowa Electronic Instruments Co., Ltd., Tokyo, Japan) were bonded using cyanoacrylate glue (Super Glue, NU Co., Ltd., Ningbo, China) to provide fast strong bonding between the model and the SG. The acetate foil (Grafix Clear Acetate, Grafix® Plastics, Maple Heights, OH, USA) served to press strain gauges firmly against the model during the glue setting. The surfaces of the models were cleaned with acetone (Aceton, Premifab d.o.o., Sveta Nedelja, Croatia) for better adhesion prior to strain gauge bonding. Strain gauges were placed as close as possible to the neck of each MDI on the vestibular and oral sides of each MDI. An additional pair of SGs was placed on the

posterior edentulous area of the mandible at sites of previous second molars, i.e., slightly anterior from the posterior end of the free-end overdenture saddles and tasked to register strains under the OD saddles during denture loading (Figure 1A,B).

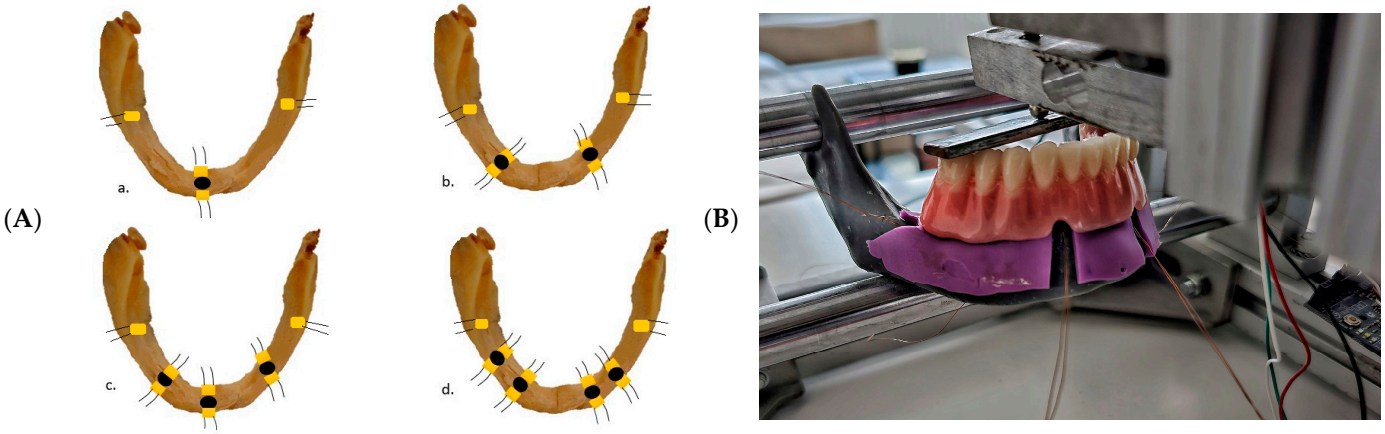

Figure 1. (**A**). Schematic drawing of the peri-implant strain gauge positions and strain gauge positions in the posterior edentulous area: (**a**). in the one-MDI model; (**b**). in the two-MDI model; (**c**). in the three-MDI model; (**d**). in the four-MDI model; (**B**). The two-MDI model mounted on the stand during bilateral overdenture loading of the mandibular overdenture in the position of the left and the right artificial first molars.

The recording system EDX-10A v02.00 (Kyowa Electronic Instruments Co., Ltd., Tokyo, Japan) was used in which all strain gauges were connected to the corresponding software program (DCS-100A v4.6, Kyowa Electronic Instruments Co., Ltd., Tokyo, Japan), which allowed simultaneous monitoring and recording of deformations during measurements.

2.5. Model Fixation

The special stand was constructed for fixation of the mandibular models to simulate the relation of the mandible to the skull (Figure 1B). Aluminum profile framework with two round bars placed horizontally supported each model on the area corresponding to the insertion of the masseter and mylohyoid muscles (lower bars), and in the mandibular notch (upper bar) (the concavity between the processus condylaris and processus coronoideus) simulating the temporomandibular joint (Figure 1B).

2.6. Overdenture Loading and Microstrain Registration

When the model was mounted on the stand, the metal screw was twisted to apply pressure on the metal plate positioned on the OD's artificial teeth, i.e., artificial molars (Figure 1B). The ODs were loaded bilaterally (Figures 1B and 2a, metal plate on the first artificial denture molars), while the screw was connected at the same time to a force-measuring cell, and the extent of the applied forces was measured. The ODs were also loaded unilaterally on the right side of the denture (unilateral loading, metal plate positioned at the right artificial first molar), and anteriorly (metal plate positioned over anterior artificial incisors; or frontal loading). As a summary, each OD was loaded in three positions: frontally (artificial incisor teeth), bilaterally (first molars on both sides of the mandible) and unilaterally (right side molar) (Figure 2a–c).

Three different forces—50 N, 100 N and 150 N—were applied during bilateral and unilateral loadings. Anterior loading was performed with only 50 N and 100 N forces. The applied forces represent average chewing forces in patients wearing overdentures supported by dental implants.

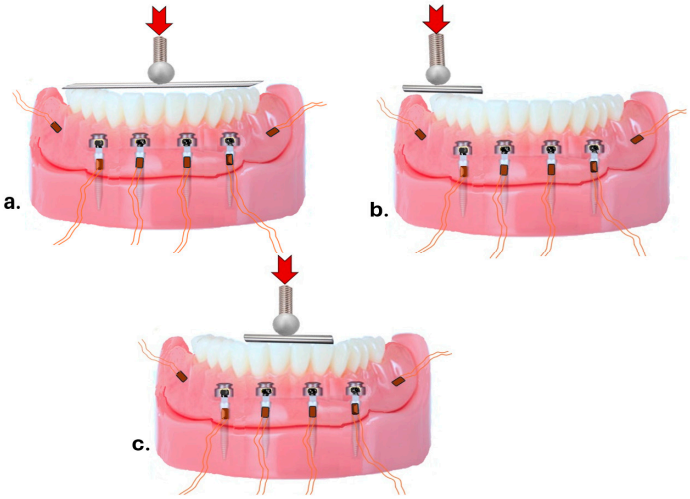

Figure 2. (**a**–**c**). Schematic drawing of loads applied to mandibular overdentures retained by one, two, three or four Ti–Zr mini-implants; (**a**). bilateral posterior OD loading in the model with four mini-implants; (**b**). unilateral posterior OD loading in the model with four mini-implants; (**c**). anterior (frontal) OD loading in the model with four mini-implants.

Microstrains were registered from the vestibular and oral peri-implant sites of each MDI, and the posterior edentulous area under OD saddles. Peri-implant strain gauges were positioned as close as possible to the implant. All loadings were performed at intervals of a few seconds until the desired loading force was achieved, which was maintained for 2 s. Microstrains in the edentulous area were recorded only under bilateral and unilateral posterior loadings. The highest registered microstrains in each of the 15 repeated measurements were entered into the database.

2.7. Statistical Analysis

Statistical analysis was performed using the SPSS 20.0 software (IBM Corporation, Armonk, NY, USA). The Shapiro–Wilks W test was used to test the normality of the distributions. The sample size calculation was done based on pilot measurements, which revealed very small variations (standard deviations ranged between 6 and 15% of the mean value). As the primary endpoint was to test the significance of the differences in loading positions and loading forces and to compare one-, two-, three-, and four-MDI models, with a presumption that the difference in the mean values will be between 15 and 30%, and with alpha set at 0.05 and a power of 80% (beta = 0.2) [30,31], the calculated sample size varied between 6 and 14 measurements. However, we decided to perform 15 measurements for each loading force and each loading position.

Mean values and standard deviations were calculated. Boxplot diagrams were also generated. The significance of the differences in the recorded peri-implant microstrains as dependent variables with the loading site and the extent of the applied forces as factors were tested using the MANOVA in each mandibular model: the one-, two-, three- and four-MDI model. The Bonferroni post-hoc test was used. The significance of the differences in the microstrains recorded from the right and left posterior edentulous area under denture saddles as dependent variables with the loading force, loading position and the number of mini-implants inserted as factors were tested using the MANOVA and Bonferroni post-hoc tests.

3. Results

Boxplot diagrams of microstrains obtained from strain gauges bonded to vestibular and oral peri-implant sites of mini-implants in the mandibular models with one, two, three and four mini-implants, dependent on loading positions and loading forces, are presented in Figures 3–6.

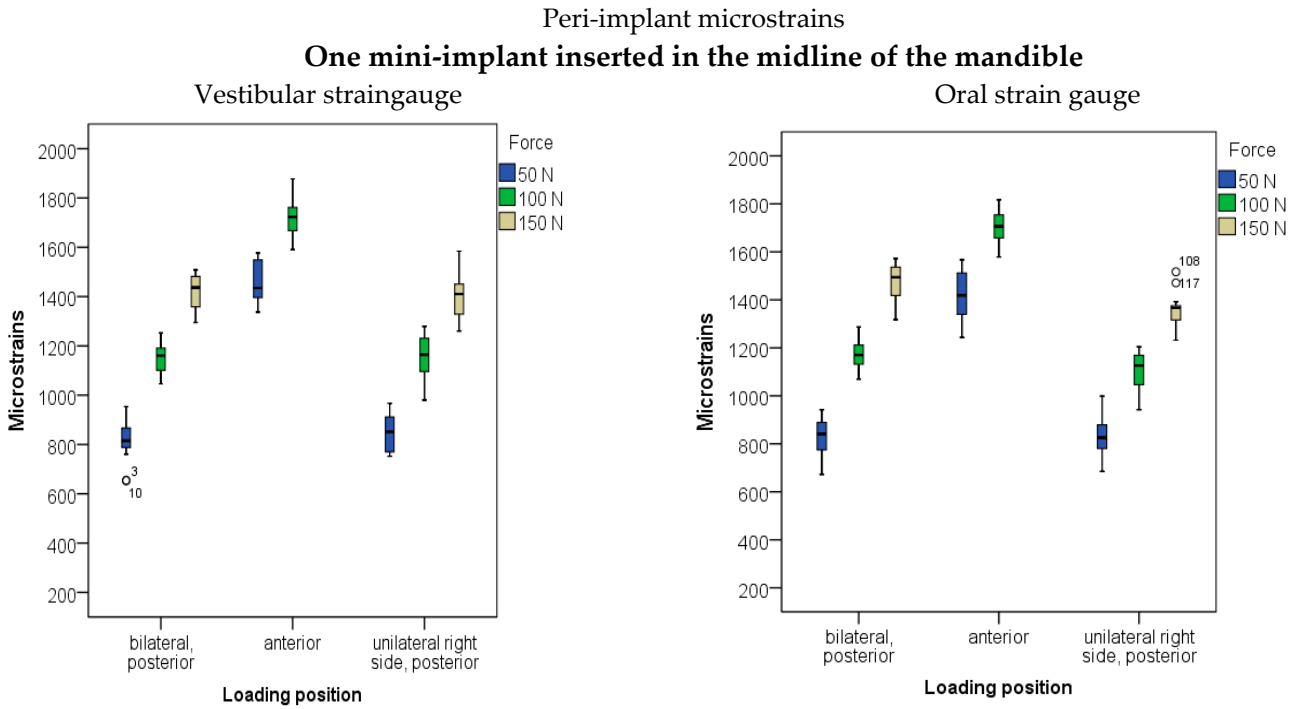

Figure 3. Boxplot diagrams of microstrains registered from strain gauges bonded to vestibular and oral peri-implant bones when only one mini-implant was inserted in the midline of the mandible.

Arithmetic means and standard deviations of microstrains obtained from strain gauges bonded to vestibular and oral peri-implant sites in the mandibular model with one MDI, dependent on the loading position and loading force, are presented in Figure 3 and Supplementary Table S1.

Arithmetic means and standard deviations of microstrains obtained from peri-implant strain gauges bonded to vestibular and oral sites of MDIs in the mandibular model with two MDIs, dependent on the loading position and loading force, are presented in Figure 4 and Supplementary Table S2.

Arithmetic means and standard deviations of microstrains obtained from peri-implant strain gauges bonded to vestibular and oral sites of MDIs in the mandibular model with three MDIs, dependent on the loading position and loading force, are presented in Figure 5 and Supplementary Table S3.

Arithmetic means and standard deviations of microstrains obtained from peri-implant strain gauges bonded to vestibular and oral sites of MDIs in the mandibular model with four MDIs, dependent on the loading position and loading force, are presented in Figure 6 and Supplementary Table S4.

When only one MDI was inserted in the midline, the highest peri-implant microstrains were recorded during anterior loading with 100 N forces from both vestibular and oral strain gauges. Posterior loadings with 150 N forces also elicited high peri-implant microstrains. The 2-factor MANOVA and Bonferroni post-hoc tests revealed that both loading forces and loading position had a significant effect on the amount of recorded peri-implant microstrains ($p < 0.001$, Supplementary Table S5a.,a.a.,a.b.).

In the two-MDI model of the mandible, the highest microstrains were recorded from the vestibular and oral SGs of the MDI on the right side of the mandible under right-side unilateral OD loading with 150 N forces. Unilateral forces elicited the highest peri-implant microstrains in the right-side MDI, followed by the left-side MDI. The MANOVA and Bonferroni post-hoc tests revealed that both loading forces and loading positions elicited statistically significant effects on the amount of recorded peri-implant microstrains in the two-MDI model ($p < 0.001$, Supplementary Table S5b.,b.a.,b.b.).

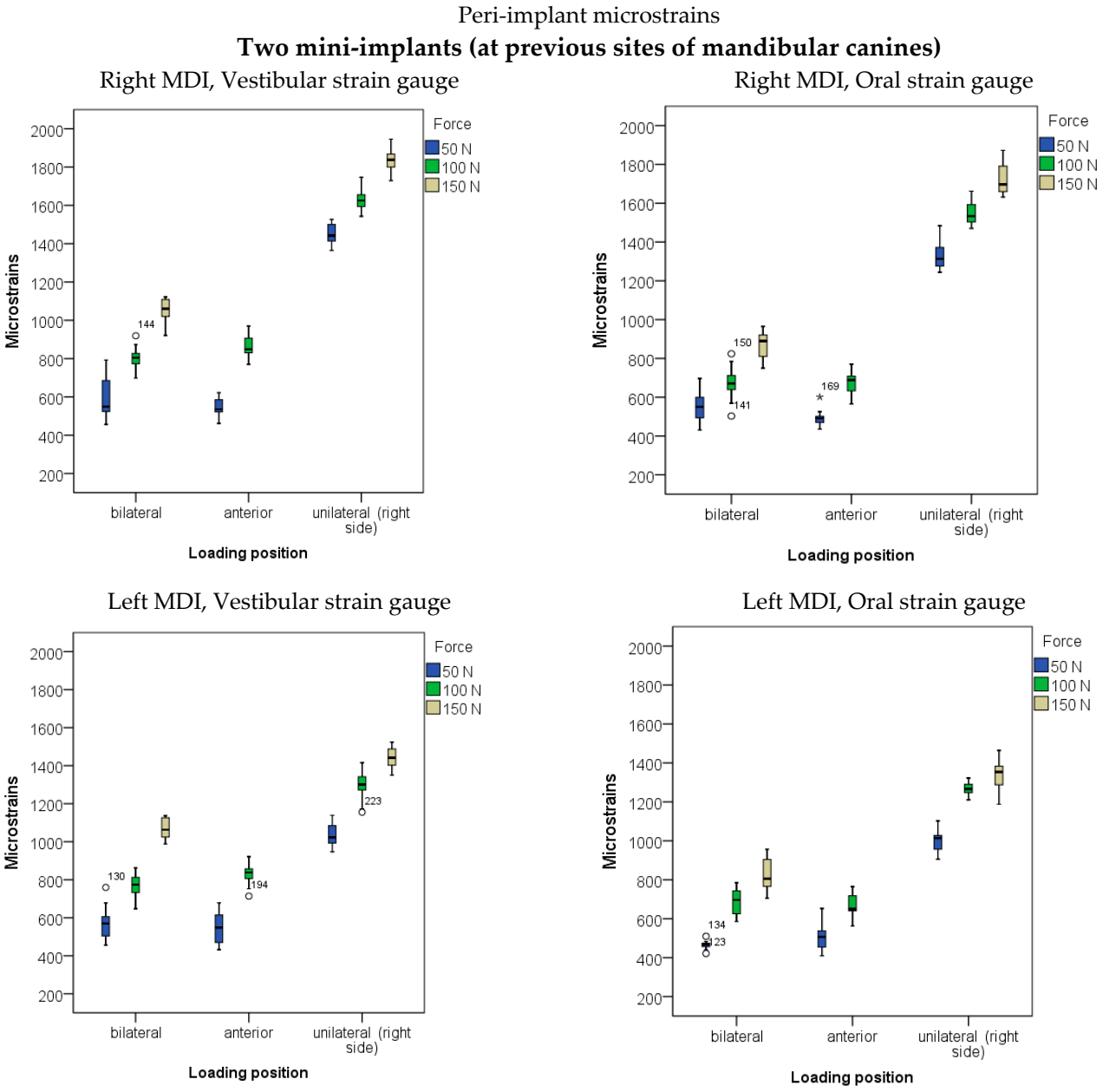

Figure 4. Boxplot diagrams of microstrains registered from strain gauges bonded to vestibular and oral peri-implant bones of two mini-implants inserted at sites previously occupied by the mandibular canines.

In the three-MDI model, the highest microstrains were recorded from the right posterior MDI under unilateral right side and bilateral loads, followed by the left MDI, while lower microstrains were recorded from the MDI inserted in the midline. The recorded microstrains were lower than in the one- and two-MDI models. The MANOVA showed significant effects of various loading forces and different loading positions on the amount of peri-implant microstrains in the three-MDI model ($p < 0.001$, Supplementary Table S5c,c.a.,c.b.).

In the four-MDI model, the highest microstrains were also recorded from the right-side posterior MDI during unilateral loading (on the right side) with the highest applied force (150 N). However, recorded microstrains were lower than in the one-, two- and even three-MDI models. Significant effects of loading positions and loading forces on peri-implant strains were shown by the MANOVA test ($p < 0.001$, Supplementary Table S5d,d.a.,d.b.).

In the two-, three- and four-MDI models, unilateral and bilateral loadings elicited significantly higher microstrains than anterior loadings. Unilateral loadings with the highest force (150 N) applied on the right side of the respective OD elicited the highest forces in the posterior right-sided MDI ($p < 0.001$).

Microstrains registered from the posterior edentulous area on the right and left sides of the mandible under mandibular overdenture saddles in the one-, two-, three-, and four-MDI overdenture models during posterior loadings are shown in boxplots in Figures 7–10 and Supplementary Table S6.

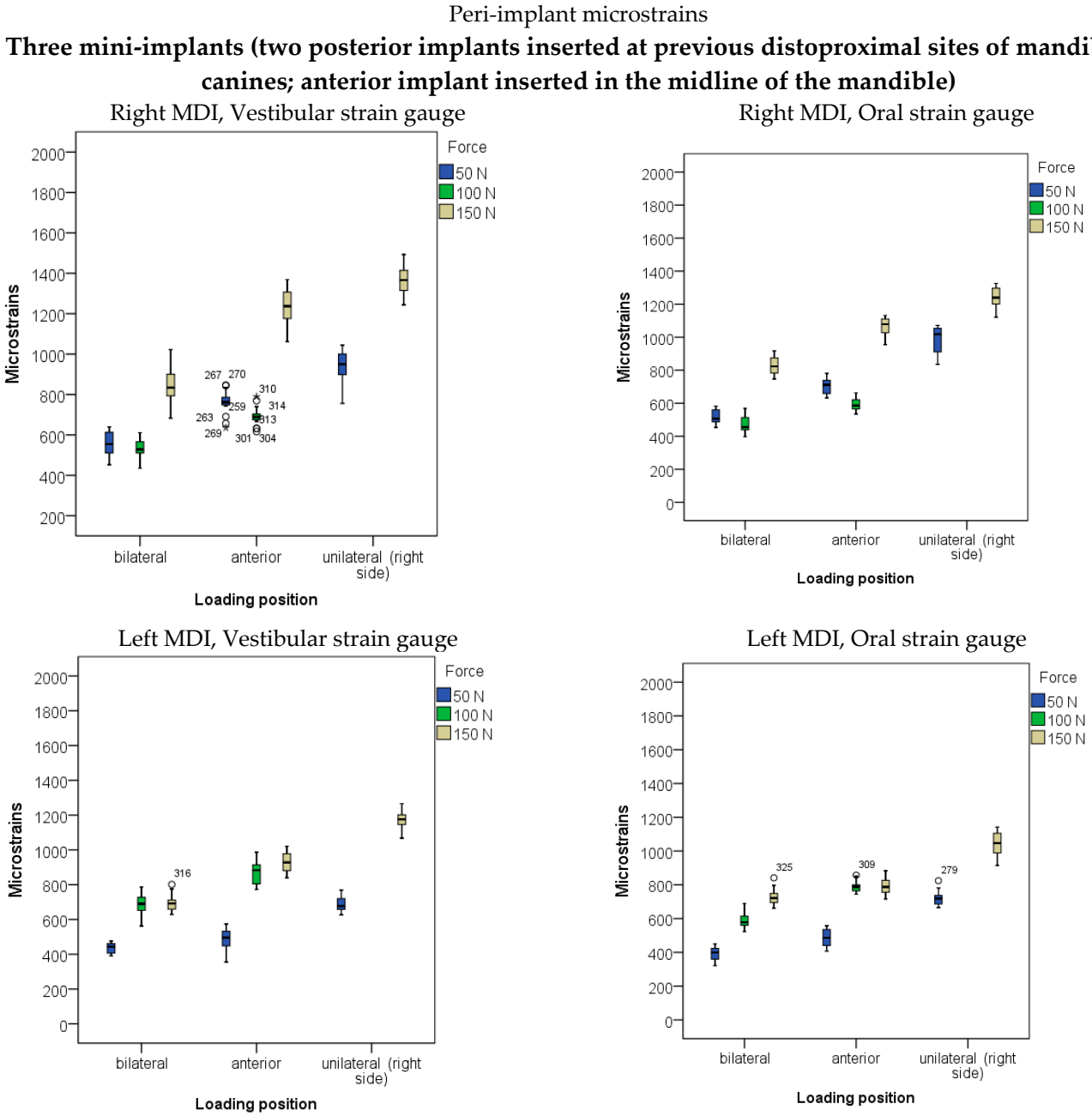

Figure 5. *Cont.*

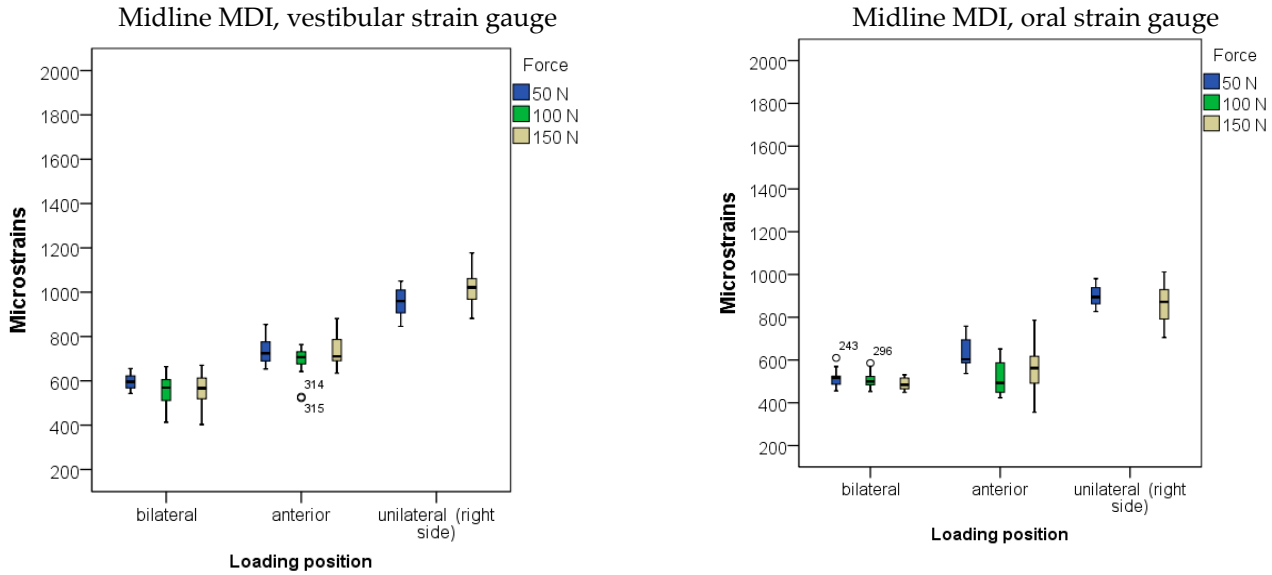

Figure 5. Boxplot diagrams of microstrains registered from peri-implant strain gauges bonded to vestibular and oral peri-implant bones when three mini-implants were inserted in the mandible; two of them were inserted in the left and right distoproximal sites of previous mandibular canines and one was inserted in the midline of the mandible.

Arithmetic means and standard deviations of microstrains obtained from strain gauges bonded to posterior edentulous areas under denture saddles during OD loading in different positions with different loading forces in the mandibular model with one MDI are presented in Figure 7 and Supplementary Table S6.

Arithmetic means and standard deviations of microstrains obtained from strain gauges bonded to posterior edentulous areas under denture saddles during OD loading in different positions with different loading forces in the mandibular model with two MDIs are presented in Figure 8 and Supplementary Table S6.

Peri-implant microstrains

Four mini-implants (two posterior implants inserted at previous first premolar sites, two anterior implants inserted at previous second incisor sites of the mandible)

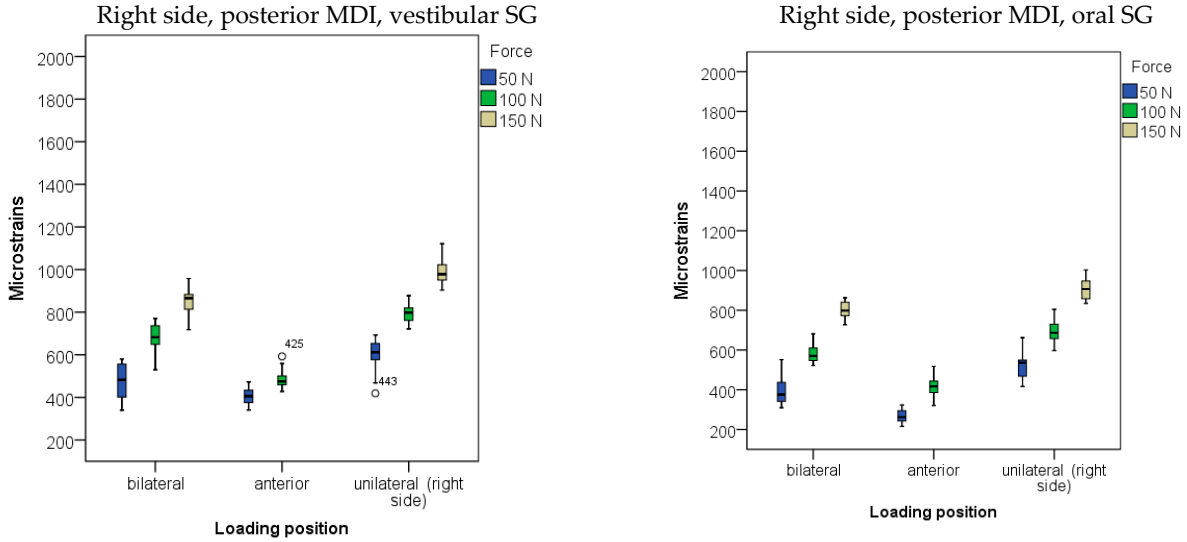

Figure 6. *Cont.*

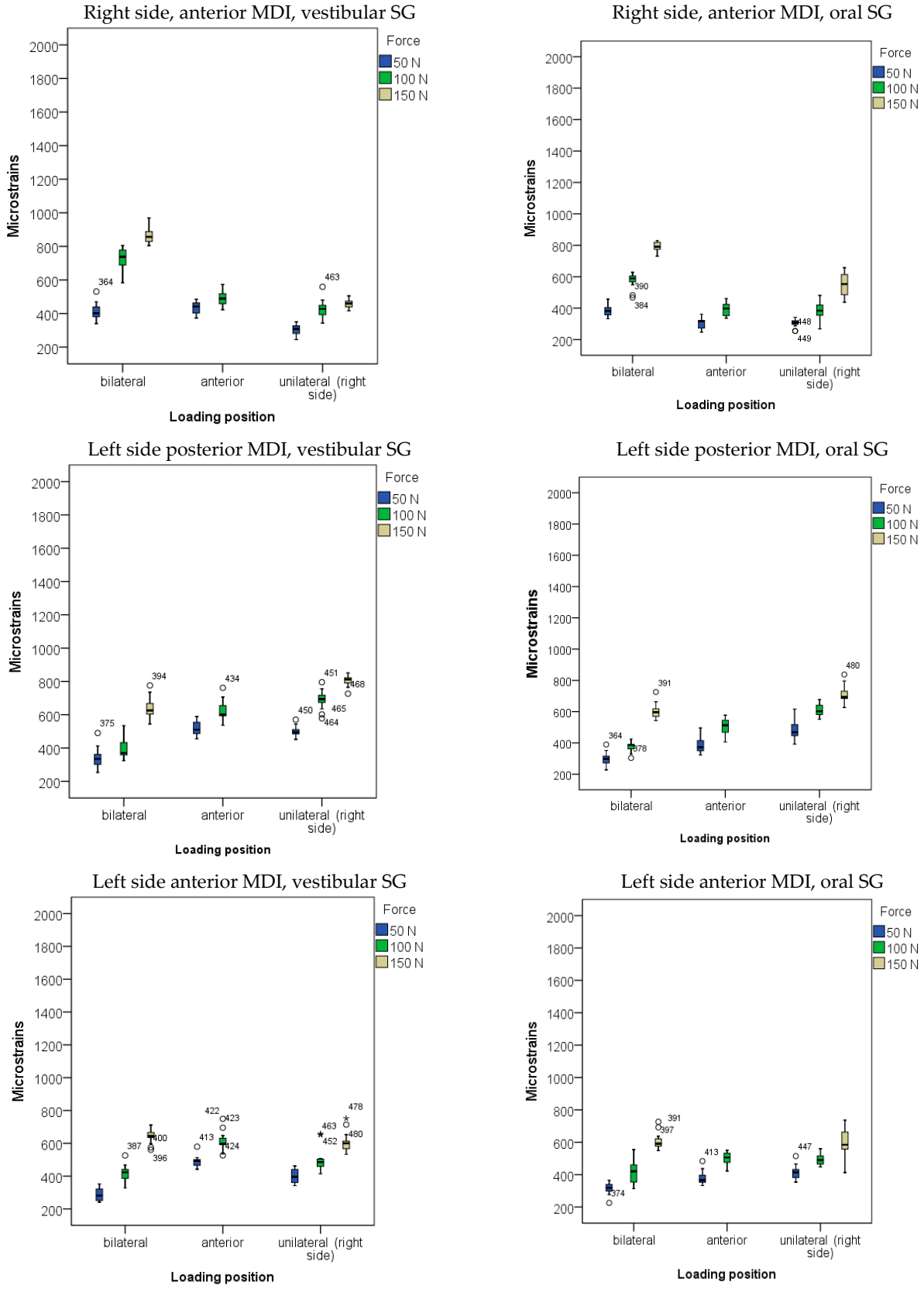

Figure 6. Boxplot diagrams of microstrains obtained from strain gauges bonded to vestibular and oral sites of peri-implant bones when four mini-implants were inserted in the mandible: two posterior mini-implants were inserted at previous first premolar sites; two anterior mini-implants were inserted at previous second incisor sites.

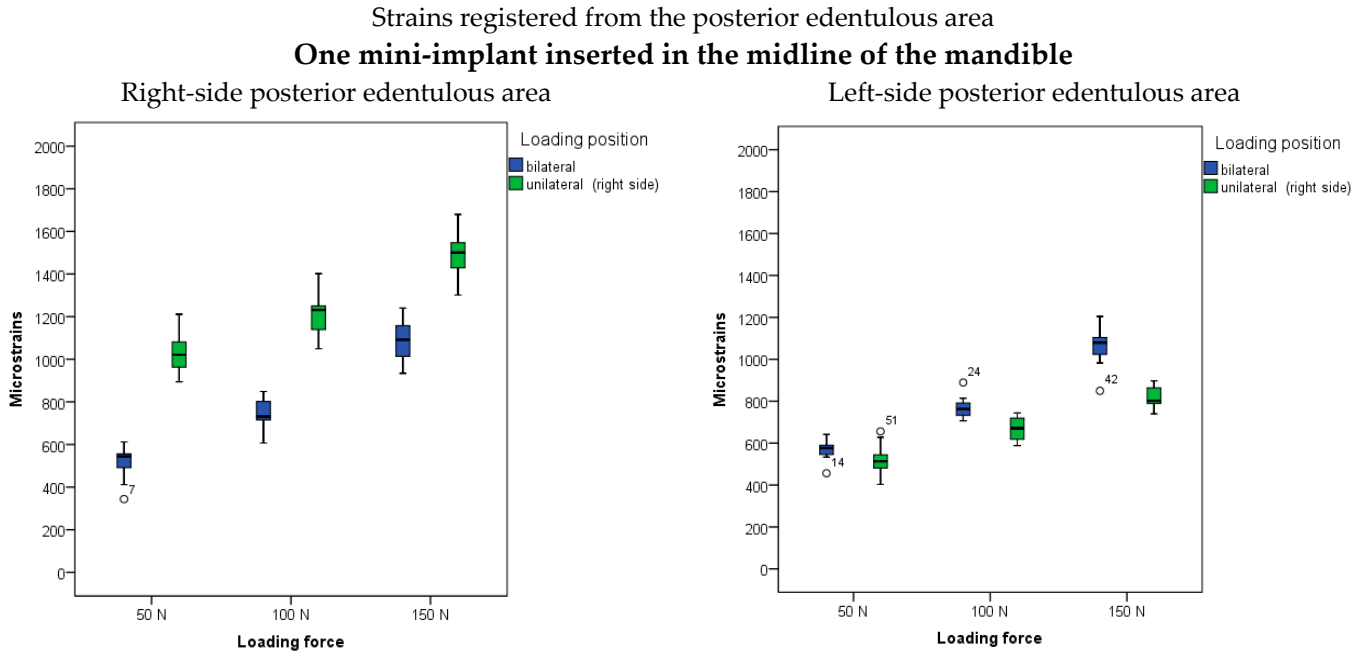

Figure 7. Microstrains registered from the right and left posterior edentulous area under mandibular overdenture saddles during posterior loading in the one-MDI model (mini-implant inserted in the midline of the mandible).

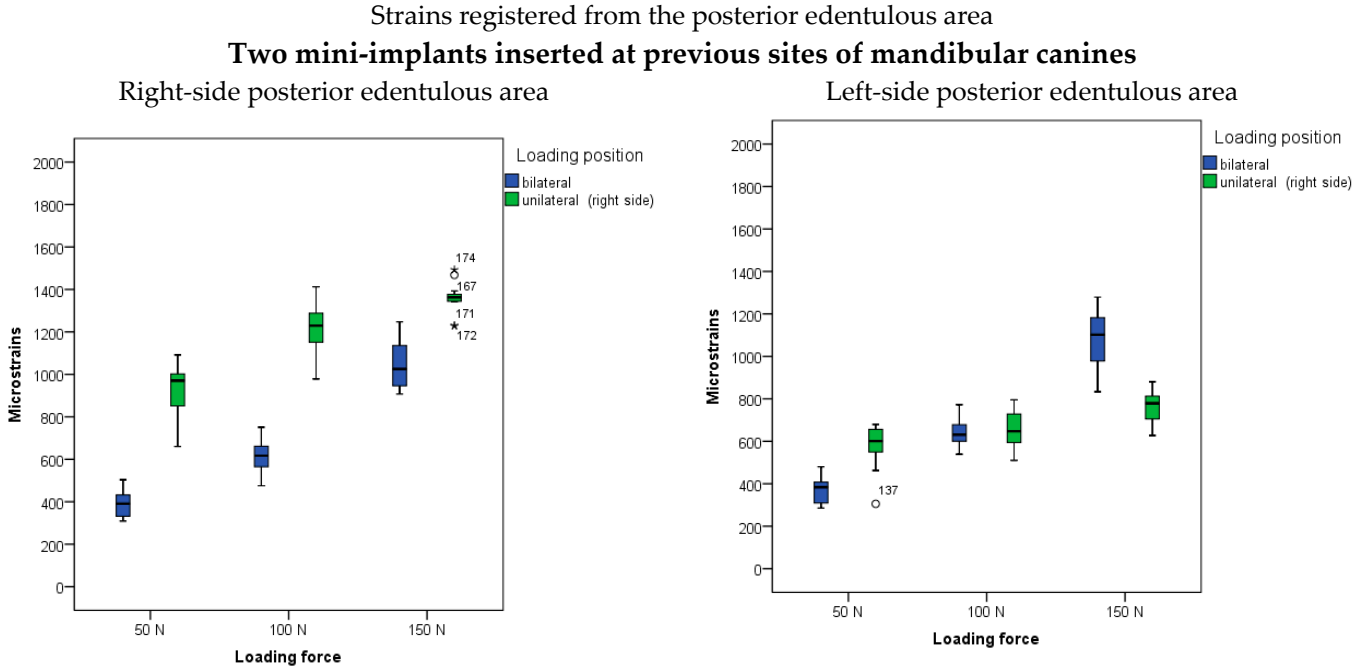

Figure 8. Microstrains registered from the right and left posterior edentulous area under mandibular overdenture saddles during posterior loadings in the two-MDI model (mini-implants inserted at previous sites of mandibular canines).

Arithmetic means and standard deviations of microstrains obtained from strain gauges bonded to posterior edentulous areas under denture saddles during OD loading in different positions with different loading forces in the mandibular model with three MDIs are presented in Figure 9 and Supplementary Table S6.

Strains registered from the posterior edentulous area

Three mini-implants; two implants inserted in previous distoproximal sites of mandibular canines, one implant inserted in the midline

Right-side posterior edentulous area

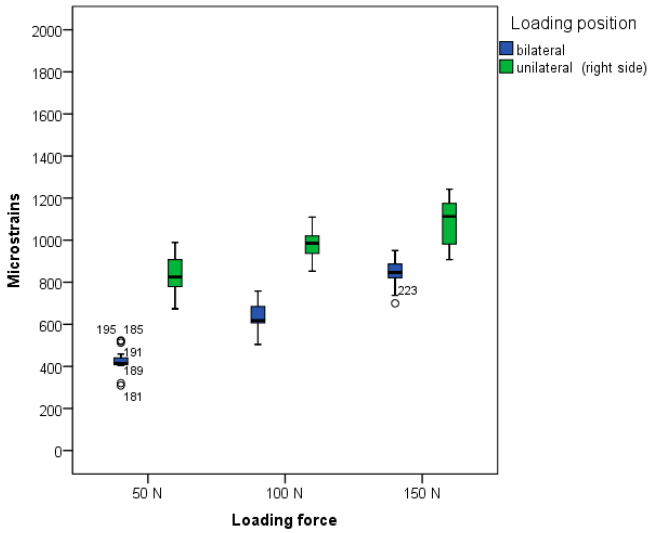

Left-side posterior edentulous area

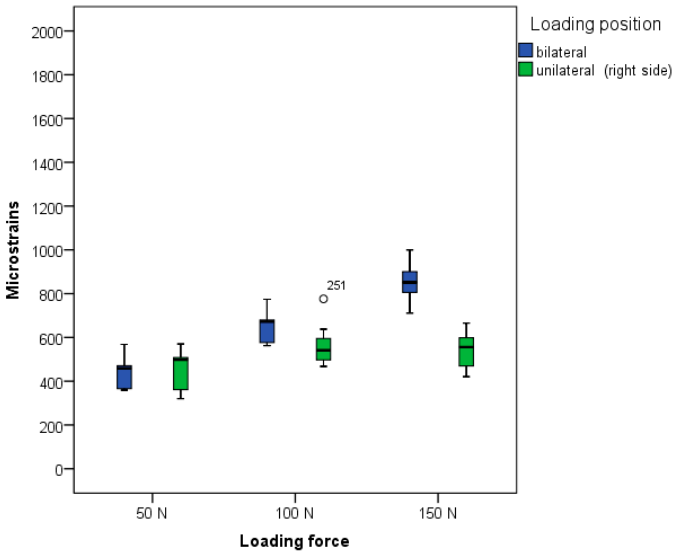

Figure 9. Microstrains registered from the right and left posterior edentulous areas under mandibular overdenture saddles during posterior loading in the three-MDI model (two mini-implants inserted in previous distoproximal sites of mandibular canines; one mini-implant inserted in the midline of the mandible).

Strains registered from the posterior edentulous area

Four mini-implants; two posterior implants inserted at previous sites of mandibular first premolars, two anterior implants inserted at previous sites of mandibular second incisors

Right-side posterior edentulous area

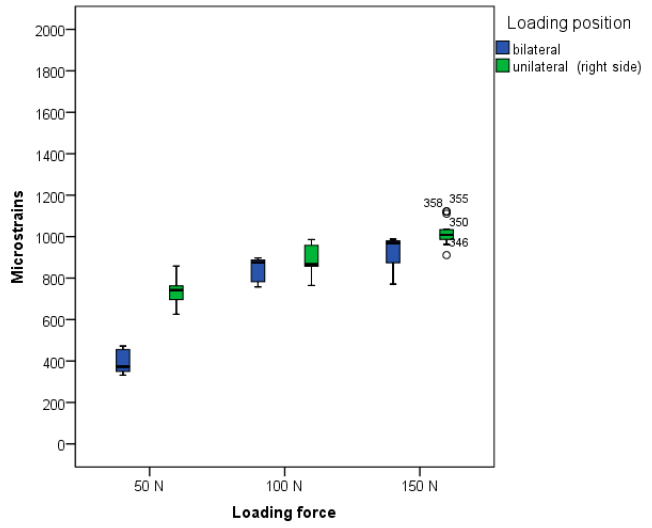

Left-side posterior edentulous area

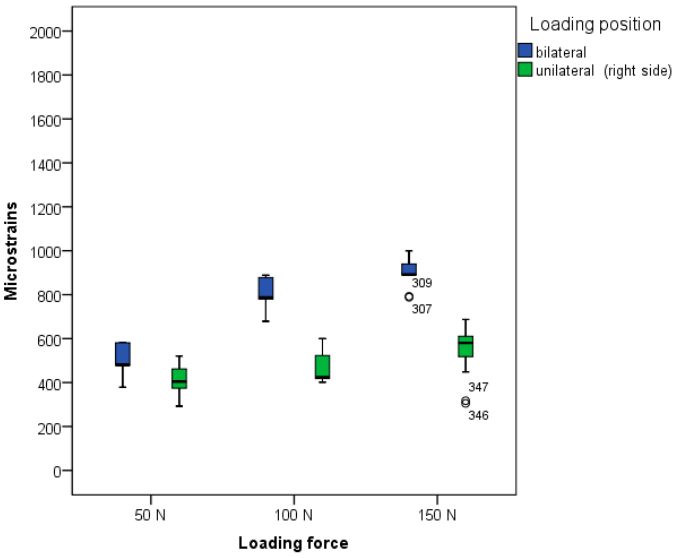

Figure 10. Microstrains registered from the right and left posterior edentulous areas under mandibular overdenture saddles during posterior loading in the four-MDI model (two mini-implants inserted at previous sites of mandibular first premolars; two mini-implants inserted at previous sites of mandibular second incisors).

Arithmetic means and standard deviations of microstrains obtained from strain gauges bonded to posterior edentulous areas under denture saddles during OD loadings in different positions with different loading forces in the mandibular model with four MDIs are presented in Figure 10 and Supplementary Table S6.

Denture settling under posterior unilateral loadings elicited the highest edentulous area strains in the one- and two-MDI models, while strains from the edentulous area under denture saddles decreased with increasing number of implants ($p > 0.001$, Supplementary Table S7). Microstrain values also increased under higher forces ($p < 0.001$).

The MANOVA and the Bonferroni post-hoc tests showed that the model was significant, and all three factors (number of MDIs, loading position and loading force) elicited significant effects ($p > 0.001$) on microstrain values registered from SGs in the posterior edentulous area during OD loading (Supplementary Table S7a–c).

4. Discussion

New materials, new techniques and dental implant modifications, as well as many other factors related to implant prosthodontic treatment innovations, need thorough in vitro investigation before their safe clinical utilization [27–29]. Due to a lack of studies on interface stress from implants on bone, which determines the strain level within the loaded bone, in vitro studies to predict clinical outcomes and marginal bone loss from peri-implant bones are crucial. Potential microfractures and bone remodeling can occur when displacement during elastic deformation exceeds 150 microns [32]. The bone first compensates for loads by forming more bone. Repeated stress with ≥3000 microstrains increases the micro-damage and can overwhelm bone reparatory mechanisms [33].

The bone bed and the MDI material do not have the same modulus of elasticity, which has a significant impact on peri-implant stress. Higher stiffness or higher elastic modulus of the implant will result in a greater amount of periimplantbone loss. Roxolid® alloy (Ti85Zr15) shows higher strength and resistance to fatigue compared to other titanium alloys [34,35]. The Roxolid® alloy amortizes part of the forces with elastic deformation during loading, thus reducing stress in the peri-implant bone [36].

Different numbers and positions of Ti90Al6V4 mini-implants supporting the mandibular OD have been studied in vitro [37]. Takagaki et al. [37] converted microstrains into lateral forces through calibration. Lateral forces were higher in the model with two MDIs inserted in the previous canine sites and in the four-MDI model compared with the one-MDI model and the two-MDI model with MDIs inserted in the positions of previous lateral second incisors. The applied loading force was only 49 N. Fewer mini-implants resulted in less lateral stress on mini-implants, which was ascribed to increased mucosal support when the number of mini-implants was reduced. However, a reduced number of implants caused a greater transfer of forces to the bearing area, resulting in a greater load on the bone. On the contrary, our study revealed lower amounts of peri-implant strains with increasing numbers of implants. Lower strains in the posterior edentulous area were recorded when more MDIs were present, which is in line with Takagaki et al. [37] (higher strains in the edentulous area with reduced numbers of implants).

Guo et al. [22] found that peri-implant microstrains were 1.5 times higher when two Ti-6Al-4V mini-implants supporting a mandibular OD (2.6 mm wide, 10 mm long) already had peri-implant marginal bone loss than when there was no marginal bone loss. The pressure on the posterior denture-bearing area was higher under the complete denture than under the two mini-implant-supported OD, as well as the displacement of the denture base. No significant differences in the posterior pressure and denture displacement were registered between MDIs with peri-implant marginal bone loss and those without marginal bone loss. Our study revealed higher strains both at the bone–implant interface and in the edentulous area in the one- and two-MDI models than in the three- and four-MDI models. Increasing the number of implants lowered the strains in the edentulous area under the same loading forces.

Warin et al. [38] emphasized a positive correlation between compressive forces and the number of implants. According to their study, the highest compressive forces were achieved with four MDIs that retained a mandibular OD, followed by three and two MDIs. In the case of bilateral loading, the compressive forces were distributed symmetrically, while in the case of unilateral loading, higher compressive forces were recorded on the side where the load was applied. With unilateral loading, a compressive force was observed on the distal side of the posterior MDI on the loaded side while a tensile force was observed on the mesial side in the model with four MDIs. Our study also revealed the highest peri-implant strains during unilateral loading (higher than during bilateral loading) on the loaded side. However, an increased number of implants led to lower peri-implant strains in our study. Bilateral loadings led to lower strains and more symmetrical strain distribution compared with unilateral loadings. We assumed that bilateral loads were equally distributed between MDIs on the left and the right sides of the mandible. Higher strains registered during posterior loadings around posterior MDIs (closer to the loading site) in the three- and four-MDI models than around anterior MDIs can be attributed to a higher extent of forces transferred to the closer implants, eliciting higher peri-implant strains on the bone. Unilateral posterior loads elicited higher strains on the loading side and in posterior implants. The highest strains recorded around the right-side implant during right-side unilateral loadings can be ascribed to the transfer of the majority of forces to the neighboring implant. As implants are stiffer than the cortical bone, strains appear in the bone near the implant–bone interface. The left side of the OD received obviously fewer loads during the unilateral loading of the OD on the right side, although microstrain peri-implant values were still high. This can be ascribed to the strong retention of the attachments of the new Ti–Zr mini-implant system (giving a denture more support) than the resilient O-ring attachment system in the Ti-6Al-4V mini-implants. Therefore, loads were transferred through the overdenture to the implants inserted on the left side. With more resilient "O" ring attachments and Ti-6Al-4V mini-implants, compressive peri-implant strains were recorded on the opposite side [38]. In the one-MDI model, the midline MDI showed the highest strains during anterior loading, even with forces of only 50 or 100 N, as the midline implant was closest to the anterior loading forces, just below the OD loading site.

It has been reported that retention force and attachment wear in mini-implant-retained ODs could be improved by increasing the mini-implant number [39–41]. Knowing that, and accounting for lower peri-implant and edentulous area strains registered in this study, we favor the utilization of three or four MDIs, especially given that the displacements and stresses are higher with mini-implants than with conventional standard-sized c-Ti implants [40].

Fatalla et al. [41] reported in their finite element analysis (FEA) that three Ti-6Al-4V MDIs retaining a mandibular OD with flexible acrylic attachments showed a lower level of Von Mises stress compared to four Ti-6Al-4V MDIs with the O-ring attachments.

Our study showed slightly lower peri-implant strains in the four-MDI model than in the three-MDI model, and almost equal strains in the posterior edentulous area, with no significant differences between the three and four new Ti–Zr MDIs for overdenture retention and support.

Very small variations in MDI insertion torque (approximately 5 Ncm) between mini-implants inserted at different sites in the models can be attributed to small differences in alveolar ridge morphology and width. The models were made from a material with characteristics of the D2 bone density, which is the most frequent in the anterior mandible between the left and right mental foramina [42].

In this study, all strain measurements were made on the models of the mandible mimicking the real patient's situation, with a favorable mucosa thickness. A height of 2 mm or less for artificial mucosa was used in other studies [37,43]. Anterior loadings were performed using 50 and 100 N, while posterior loadings were performed using 50, 100 and 150 N forces due to the fact that the magnitude of chewing forces in the anterior region

are lower than in the premolar and molar regions [44]. The extent of loading forces [45] applied in this study represents average chewing forces in subjects with implant-supported ODs [46]. Chewing forces are lower in conventional complete dentures and vary from 30 to 50 N [46], but are much higher in subjects with their own teeth or fixed partial dentures [44].

The differences between the results of this study and other studies on biomechanical behavior [37,38,47–54] may be due to different mini-implant materials (Ti–Zr vs. Ti-Al6-V4), different retention mechanisms (Optiloc® Retentive System vs. "O"-ring), different implant designs and neck widths [55], different dimensions of implants [56,57], small differences in strain measurements and different residual ridge forms. We bonded strain gauges as close as possible to the implant–bone interface due to the assumption that stress and strains would be highest where two materials with different stiffnesses meet. The cyanoacrylate glue was recommended by the strain gauge manufacturer and was also used in other studies utilizing SGs. Some experimental results indicate that SGs used with the same adhesive gave consistent deformation values, while different glues (cyanoacrylate, epoxy) led to different values under the same conditions [58]. Therefore, it is important to use the same glue as in other similar studies to be able to compare the results. Moreover, the adhesive thickness should be the lowest possible and should be uniformly applied. A linear relationship between adhesive thickness and strain error has been found [58]. For this reason, we used acetate foil to firmly press strain gauges against the model during the glue setting to have the thinnest possible glue layer. One of the limitations of this study is that we could not control the glue thickness completely.

The new Ti–Zr (Roxolid®) Mini-Implant system utilizes binary titanium alloy with approximately 15% Zr, which is an α alloy with a closely packed hexagonal crystallographic structure and represents a completely solid solution [35,36,59], contrary to Ti-6Al-4V trinary alloy, which consists of α and β phases (closely packed hexagonal and body-centered cubic crystals) [59,60]. A solid solution of a Ti–Zr alloy allows better and faster cell adhesion and faster and better osseointegration. There is no degradation of potentially cytotoxic vanadium. However, both alloys have similar mechanical properties [59,60]. An elastic modulus of the Roxolid® alloy is reported to be 96.12 ± 2.82 GPa, significantly lower than that of titanium [60], while according to Brizuela et al. [35,36] it varies between 102 and 104.7 GPa, with a Poisson coefficient of 0.33. The Roxolid® alloy has similar elastic characteristics to the Ti-6Al-4V alloy (110–115 GPa) but with a higher tensile strength [35,36]. The cortical bone modulus of elasticity is only 15 GPa [35,36]. The hardness value of Ti by nanoindentation was 2.38 ± 0.13 GPa and that of Ti–Zr Roxolid® alloy was 3.19 ± 0.09 GPa [60]. Medvedev et al. [61] reported the yield strength of the Roxolid® alloy to be 799 ± 26 MPa, and the ultimate tensile strength to be 968 ± 2.6, higher than that of grade four Ti, but similar to that of the Ti-6Al-4V alloy (970 MPa). The data on the mechanical properties of these alloys show a certain amount of variability, as reported in different studies [62]. All microstrains reported in this study represented the peak (maximum) microstrains during the two-second OD loading interval after the desired loading force had been achieved. The maximum strain values during the 2 s loading period were chosen because the applied force varied by a very small amount during the 2 s. Additionally, repeated strains can interfere with bone reparatory mechanisms even in the range of 1500–3000, which corresponds to mild overloads [33]. However, none of the maximum microstrains registered in the present study exceeded a value of 3000, when bone reparatory mechanisms can be jeopardized. However, in a real patient situation, chewing forces can be greater than in this study [44,45], especially in subjects with natural teeth in the maxilla and in those with bruxing habits. Due to the fact that microstrains increase under higher loading forces, higher chewing forces may elicit higher strains in a real patient situation compared with this study, especially when keeping in mind that the magnitude of chewing forces is inversely correlated with proprioception [44]. Moreover, in a real clinical situation, the attached mucosa is not of uniform thickness and consistency. Various mucosal thicknesses can be found at different alveolar ridge sites in the same subject. Sometimes even a flabby ridge can be present. All these complicate denture micromovements under loads, and thus the direction and distri-

bution of the transferred forces. Therefore, higher strains can be elicited in a real-patient situation compared with those recorded in the present study, or strains can be repeated more frequently. Additionally, implant inclination (parallel in this study) may be different in a real-patient situation due to the morphology of the alveolar bone, and all this can influence the distribution of loads and consequent strains in the peri-implant and posterior edentulous area bone. The bone density in real patients can be lower than the D2 density in this study, which would lead to a larger difference in the elasticity modulus between the implant and the bone, as the low-density bone has a lower elasticity modulus than the cortical bone. We mimicked a near-ideal patient situation. Therefore, the aforementioned facts represent the study's limitations and should be addressed in future research.

Because high strains were recorded during anterior loading in the one-MDI model, even under small forces, the utmost precaution should be taken in such clinical situations due to the possibility of implant overloading under higher forces and more unfavorable alveolar ridge morphology, lower bone density or mucosa thickness. In subjects with two MDIs, the highest strains were recorded under unilateral 150 N loads. Strains may be even higher under higher OD loading forces and in less favorable clinical situations (uneven mucosal heights and consistency, lower bone density, etc.). Therefore, it is very important to advise patients to chew bilaterally, especially when a low number of implants is present. In the three- and four-MDI models, peri-implant and edentulous area strains were far from those that could interfere with the bone reparatory mechanisms. Therefore, three or four Ti–Zr mini-implants can be used clinically for retention of mandibular OD without too much fear of failure. Additionally, the dimensions of implants [56,57], mucosa thickness, height and consistency, residual ridge morphology, bone density, overdenture characteristics, and extent and direction of chewing forces [44–46] play an important role in stress and strain distribution. Therefore, future studies are needed to complete the overview of mandibular overdentures retained by Ti–Zr mini-implants.

The limitation of the study is that the models represent only an average case scenario of possible situations in a "real" mouth. However, higher loading forces, different thicknesses and consistencies of the mucosa and inclination of MDIs could lead to different results and should be studied further. We also could not fully control all parameters, e.g., glue thickness, as SGs were manually bonded. Different bone densities could also influence the results and should be studied further. Additionally, the elastic modulus of a metal plate transferring loads to ODs could influence the results.

The strength is that this study is the first one to analyze the new mini-implant system made from the Roxolid® (Ti–Zr) dental alloy with a new innovative retention mechanism (Optiloc® Retentive System) when varying the number of inserted implants for retention and support of mandibular ODs.

5. Conclusions

Within the limitations of the study, we can arrive at the conclusion that the increased number of MDIs reduces the amount of microstrains around implants and in the posterior edentulous area. The highest microstrains were achieved under 150 N forces and unilateral loading in the two-MDI model. In the one-MDI model, anterior loading with both 50 and 100 N elicited higher peri-implant microstrains than posterior loads. Posterior loads elicited higher peri-implant microstrains around the posterior than anterior MDIs. Unilateral loadings elicited higher strains than bilateral loads, especially in implants on the loaded side. In the posterior edentulous areas, the highest microstrains were recorded in the one- and two-MDI models. Although none of the recorded strains interfered with bone reparatory mechanisms, precautions should be taken, and additional investigations should be conducted for the one- and two-MDI models.

Supplementary Materials: The following supporting information can be downloaded at: https://www.mdpi.com/article/10.3390/app14052150/s1.

Author Contributions: Conceptualization, N.P. and A.C.; methodology, I.K., D.P., A.C. and N.P.; writing—original draft preparation, D.P. and I.K.; writing—reviewing and editing, N.P. and A.C.; Data analysis: A.C.; Data Interpretation: A.C., N.P., D.P. and I.K.; funding acquisition: N.P. and A.C. All authors have read and agreed to the published version of the manuscript.

Funding: This research received no external funding.

Data Availability Statement: The raw data supporting the conclusions in this article are available from the authors on request.

Acknowledgments: The authors thank the Institut Straumann AG for the donation of the Ti–Zr (Roxolid®) alloy mini-implants used in this study.

Conflicts of Interest: The authors declare that this study received funding from Institut Straumann AG. The funder was not involved in the study design, collection, analysis, interpretation of data, the writing of this article or the decision to submit it for publication.

References

1. Marcello-Machado, R.M.; Faot, F.; Schuster, A.J.; Nascimento, G.G.; Del Bel Cury, A.A. Mini-Implants and Narrow Diameter Implants as Mandibular Overdenture Retainers: A Systematic Review and Meta-Analysis of Clinical and Radiographic Outcomes. *J. Oral Rehabil.* **2018**, *45*, 161–183. [CrossRef]
2. Topić, J.; Poljak-Guberina, R.; Persic-Kirsic, S.; Kovacic, I.; Petricevic, N.; Popovac, A.; Čelebić, A. Adaptation to New Dentures and 5 Years of Clinical Use: A Comparison between Complete Denture and Mini-Implant Mandibular Overdenture Patients Based on Oral Health-Related Quality of Life (OHRQoL) and Orofacial Esthetics. *Acta Stomatol. Croat.* **2022**, *56*, 132–142. [CrossRef]
3. Čelebić, A.; Peršić, S.; Kovačić, I.; Buković, D.; Lešić, N.; Rener-Sitar, K. Comparison of Three Prosthodontic Treatment Modalities for Patients with Periodontally Compromised Anterior Mandibular Teeth: A 2-Year Follow-up Study. *Acta Stomatol. Croat.* **2019**, *53*, 4–16. [CrossRef]
4. Elsyad, M.A.; Gebreel, A.A.; Fouad, M.M.; Elshoukouki, A.H. The Clinical and Radiographic Outcome of Immediately Loaded Mini Implants Supporting a Mandibular Overdenture. A 3-Year Prospective Study: CLINICAL AND RADIOGRAPHIC OUTCOME OF MINI IMPLANTS. *J. Oral Rehabil.* **2011**, *38*, 827–834. [CrossRef]
5. Kovačić, I.; Peršić, S.; Kranjčić, J.; Čelebić, A. A Cohort Study on Short Mini-implants for Mandibular Overdentures Compared to Those of Standard Length. *Clin. Oral Implant. Res.* **2020**, *31*, 121–132. [CrossRef]
6. Schimmel, M.; Janner, S.F.M.; Joda, T.; Wittneben, J.G.; McKenna, G.; Brägger, U. Mandibular Implant-Supported Fixed Complete Dental Prostheses on Implants with Ultrashort and Standard Length: A Pilot Treatment. *J. Prosthet. Dent.* **2021**, *126*, 137–143. [CrossRef]
7. Enkling, N.; Haueter, M.; Worni, A.; Müller, F.; Leles, C.R.; Schimmel, M. A Prospective Cohort Study on Survival and Success of One-Piece Mini-Implants with Associated Changes in Oral Function: Five-Year Outcomes. *Clin. Oral Implant. Res.* **2019**, *30*, 570–577. [CrossRef]
8. AlHelal, A.A. Application of Immediate Loaded Mini Dental Implants for Retaining Mandibular Overdenture Prosthesis in Edentulous Patients: A Systematic Review. *Appl. Sci.* **2021**, *11*, 10724. [CrossRef]
9. Rosa, A.; Pujia, A.M.; De Angelis, R.; Arcuri, C. Narrow Implants and Overdentures in the Total Rehabilitation of Atrophic Edentulous Jaws: Review of Clinical Aspects with Meta-Analysis. *Prosthesis* **2023**, *6*, 41–52. [CrossRef]
10. Peršić, S.; Ćelić, R.; Vojvodić, D.; Petričević, N.; Kranjčić, J.; Zlatarić, D.K.; Čelebić, A. Oral Health-Related Quality of Life in Different Types of Mandibular Implant Overdentures in Function Longer Than 3 Years. *Int. J. Prosthodont.* **2016**, *29*, 28–30. [CrossRef]
11. Feine, J.S.; Carlsson, G.E.; Awad, M.A.; Chehade, A.; Duncan, W.J.; Gizani, S.; Head, T.; Heydecke, G.; Lund, J.P.; MacEntee, M.; et al. The McGill Consensus Statement on Overdentures. Mandibular Two-Implant Overdentures as First Choice Standard of Care for Edentulous Patients. *Gerodontology* **2002**, *19*, 3–4.
12. Jung, R.E.; Al-Nawas, B.; Araujo, M.; Avila-Ortiz, G.; Barter, S.; Brodala, N.; Chappuis, V.; Chen, B.; De Souza, A.; Almeida, R.F.; et al. Group 1 ITI Consensus Report: The Influence of Implant Length and Design and Medications on Clinical and Patient-Reported Outcomes. *Clin. Oral Implant. Res.* **2018**, *29* (Suppl. S16), 69–77. [CrossRef] [PubMed]
13. Goiato, M.C.; Sônego, M.V.; Pellizzer, E.P.; Gomes, J.M.d.L.; da Silva, E.V.F.; Dos Santos, D.M. Clinical Outcome of Removable Prostheses Supported by Mini Dental Implants. A Systematic Review. *Acta Odontol. Scand.* **2018**, *76*, 628–637. [CrossRef] [PubMed]
14. Park, J.-H.; Lee, J.-Y.; Shin, S.-W. Treatment Outcomes for Mandibular Mini-Implant–Retained Overdentures: A Systematic Review. *Int. J. Prosthodont.* **2017**, *30*, 269–276. [CrossRef]
15. Celebic, A.; Kovacic, I.; Petricevic, N.; Alhajj, M.N.; Topic, J.; Junakovic, L.; Persic-Kirsic, S. Clinical Outcomes of Three versus Four Mini-Implants Retaining Mandibular Overdenture: A 5-Year Randomized Clinical Trial. *Medicina* **2023**, *60*, 17. [CrossRef]
16. Al Jaghsi, A.; Heinemann, F.; Biffar, R.; Mundt, T. Immediate versus Delayed Loading of Strategic Mini-Implants under Existing Removable Partial Dentures: Patient Satisfaction in a Multi-Center Randomized Clinical Trial. *Clin. Oral Investig.* **2021**, *25*, 255–264. [CrossRef] [PubMed]

17. Mundt, T.; Heinemann, F.; Müller, J.; Schwahn, C.; Al Jaghsi, A. Survival and Stability of Strategic Mini-Implants with Immediate or Delayed Loading under Removable Partial Dentures: A 3-Year Randomized Controlled Clinical Trial. *Clin. Oral Investig.* **2022**, *27*, 1767–1779. [CrossRef]
18. Celebic, A.; Kovacic, I.; Petricevic, N.; Puljic, D.; Popovac, A.; Kirsic, S.P. Mini-Implants Retaining Removable Partial Dentures in Subjects without Posterior Teeth: A 5-Year Prospective Study Comparing the Maxilla and the Mandible. *Medicina* **2023**, *59*, 237. [CrossRef]
19. Catalán, A.; Martínez, A.; Marchesani, F.; González, U. Mandibular Overdentures Retained by Two Mini-Implants: A Seven-Year Retention and Satisfaction Study. *J. Prosthodont.* **2016**, *25*, 364–370. [CrossRef]
20. Bellia, E.; Boggione, L.; Terzini, M.; Manzella, C.; Menicucci, G. Immediate Loading of Mandibular Overdentures Retained by Two Mini-Implants: A Case Series Preliminary Report. *Int. J. Prosthodont.* **2018**, *31*, 558–564. [CrossRef]
21. Jofre, J.; Cendoya, P.; Munoz, P. Effect of Splinting Mini-Implants on Marginal Bone Loss: A Biomechanical Model and Clinical Randomized Study with Mandibular Overdentures. *Int. J. Oral Maxillofac. Implant.* **2010**, *25*, 1137–1144.
22. Guo, Y.; Kono, K.; Suzuki, Y.; Ohkubo, C.; Zeng, J.-Y.; Zhang, J. Influence of Marginal Bone Resorption on Two Mini Implant-Retained Mandibular Overdenture: An in Vitro Study. *J. Adv. Prosthodont.* **2021**, *13*, 55–64. [CrossRef]
23. Coskunses, F.M.; Tak, Ö. Clinical Performance of Narrow-Diameter Titanium–Zirconium Implants in Immediately Loaded Fixed Full-Arch Prostheses: A 2-Year Clinical Study. *Int. J. Implant. Dent.* **2021**, *7*, 30. [CrossRef] [PubMed]
24. Badran, Z.; Struillou, X.; Strube, N.; Bourdin, D.; Dard, M.; Soueidan, A.; Hoornaert, A. Clinical Performance of Narrow-Diameter Titanium-Zirconium Implants: A Systematic Review. *Implant. Dent.* **2017**, *26*, 316–323. [CrossRef] [PubMed]
25. Cao, R.; Chen, B.; Xu, H.; Fan, Z. Clinical Outcomes of Titanium-Zirconium Alloy Narrow-Diameter Implants for Single-Crown Restorations: A Systematic Review and Meta-Analysis. *Br. J. Oral Maxillofac. Surg.* **2023**, *61*, 403–410. [CrossRef] [PubMed]
26. Curado, T.F.F.; Silva, J.R.; Nascimento, L.N.; Leles, J.L.R.; McKenna, G.; Schimmel, M.; Leles, C.R. Implant Survival/Success and Peri-Implant Outcomes of Titanium-Zirconium Mini Implants for Mandibular Overdentures: Results from a 1-Year Randomized Clinical Trial. *Clin. Oral Implant. Res.* **2023**, *34*, 769–782. [CrossRef] [PubMed]
27. Rani, I.; Shetty, J.; Reddy, V. A Comparison of Peri-Implant Strain Generated by Different Types of Implant Supported Prostheses. *J. Indian. Prosthodont. Soc.* **2017**, *17*, 142. [CrossRef]
28. Wang, P.-S.; Tsai, M.-H.; Wu, Y.-L.; Chen, H.-S.; Lei, Y.-N.; Wu, A.Y.-J. Biomechanical Analysis of Titanium Dental Implants in the All-on-4 Treatment with Different Implant–Abutment Connections: A Three-Dimensional Finite Element Study. *J. Funct. Biomater.* **2023**, *14*, 515. [CrossRef]
29. Chakraborty, A.; Datta, P.; Kumar, C.S.; Majumder, S.; Roychowdhury, A. Probing Combinational Influence of Design Variables on Bone Biomechanical Response around Dental Implant-supported Fixed Prosthesis. *J. Biomed. Mater. Res.* **2022**, *110*, 2338–2352. [CrossRef]
30. Julious, S.A. Sample Size of 12 per Group Rule of Thumb for a Pilot Study. *Pharm. Stat.* **2005**, *4*, 287–291. [CrossRef]
31. Gupta, K.; Attri, J.; Singh, A.; Kaur, H.; Kaur, G. Basic Concepts for Sample Size Calculation: Critical Step for Any Clinical Trials! *Saudi J. Anaesth.* **2016**, *10*, 328. [CrossRef] [PubMed]
32. Szmukler-Moncler, S.; Salama, H.; Reingewirtz, Y.; Dubruille, J.H. Timing of Loading and Effect of Micromotion on Bone-Dental Implant Interface: Review of Experimental Literature. *J. Biomed. Mater. Res.* **1998**, *43*, 192–203. [CrossRef]
33. Frost, H.M. A 2003 Update of Bone Physiology and Wolff's Law for Clinicians. *Angle Orthod* **2004**, *74*, 3–15. [CrossRef] [PubMed]
34. Ho, W.-F.; Chen, W.-K.; Wu, S.-C.; Hsu, H.-C. Structure, Mechanical Properties, and Grindability of Dental Ti-Zr Alloys. *J. Mater. Sci. Mater. Med.* **2008**, *19*, 3179–3186. [CrossRef] [PubMed]
35. Brizuela, A.; Herrero-Climent, M.; Rios-Carrasco, E.; Rios-Santos, J.; Pérez, R.; Manero, J.; Gil Mur, J. Influence of the Elastic Modulus on the Osseointegration of Dental Implants. *Materials* **2019**, *12*, 980. [CrossRef] [PubMed]
36. Brizuela-Velasco, A.; Pérez-Pevida, E.; Jiménez-Garrudo, A.; Gil-Mur, F.J.; Manero, J.M.; Punset-Fuste, M.; Chávarri-Prado, D.; Diéguez-Pereira, M.; Monticelli, F. Mechanical Characterisation and Biomechanical and Biological Behaviours of Ti-Zr Binary-Alloy Dental Implants. *Biomed. Res. Int.* **2017**, *2017*, 2785863. [CrossRef] [PubMed]
37. Takagaki, K.; Gonda, T.; Maeda, Y. Number and Location of Mini-Implants Retaining a Mandibular Overdenture to Resist Lateral Forces: A Preliminary In Vitro Study. *Int. J. Prosthodont.* **2017**, *30*, 248–250. [CrossRef] [PubMed]
38. Warin, P.; Rungsiyakull, P.; Rungsiyakull, C.; Khongkhunthian, P. Effects of Different Numbers of Mini-Dental Implants on Alveolar Ridge Strain Distribution under Mandibular Implant-Retained Overdentures. *J. Prosthodont. Res.* **2018**, *62*, 35–43. [CrossRef]
39. Alshenaiber, R.; Silikas, N.; Barclay, C. Does the Length of Mini Dental Implants Affect Their Resistance to Failure by Overloading? *Dent. J.* **2022**, *10*, 117. [CrossRef]
40. Lohmann, A.; Keilig, L.; Heinemann, F.; Bourauel, C.; Hasan, I. Numerical Investigation of Complete Mandibular Dentures Stabilized by Conventional or Mini Implants in Patient Individual Models. *Biomed. Eng./Biomed. Tech.* **2019**, *64*, 103–110. [CrossRef]
41. Fatalla, A.A.; Song, K.; Du, T.; Cao, Y. A Three-Dimensional Finite Element Analysis for Overdenture Attachments Supported by Teeth and/or Mini Dental Implants. *J. Prosthodont.* **2012**, *21*, 604–613. [CrossRef]
42. Hao, Y.; Zhao, W.; Wang, Y.; Yu, J.; Zou, D. Assessments of Jaw Bone Density at Implant Sites Using 3D Cone-Beam Computed Tomography. *Eur. Rev. Med. Pharmacol. Sci.* **2014**, *18*, 1398–1403. [PubMed]

43. Elsyad, M.A.; Setta, F.A.; Khirallah, A.S. Strains around Distally Inclined Implants Retaining Mandibular Overdentures with Locator Attachments: An In Vitro Study. *J. Adv. Prosthodont.* **2016**, *8*, 116. [CrossRef] [PubMed]
44. Atlas, A.M.; Behrooz, E.; Barzilay, I. Can Bite-Force Measurement Play a Role in Dental Treatment Planning, Clinical Trials, and Survival Outcomes? A Literature Review and Clinical Recommendations. *Quintessence Int.* **2022**, *53*, 632–642. [CrossRef] [PubMed]
45. Van Der Bilt, A.; Burgers, M.; Van Kampen, F.M.C.; Cune, M.S. Mandibular Implant-supported Overdentures and Oral Function. *Clin. Oral Implant. Res.* **2010**, *21*, 1209–1213. [CrossRef]
46. Fayad, M.; Alruwaili, H.T.; Khan, M.; Baig, M. Bite Force Evaluation in Complete Denture Wearer with Different Denture Base Materials: A Randomized Controlled Clinical Trial. *J. Int. Soc. Prevent. Community Dent.* **2018**, *8*, 416. [CrossRef] [PubMed]
47. Patil, P.G.; Seow, L.L.; Uddanwadikar, R.; Ukey, P.D. Biomechanical Behavior of Mandibular Overdenture Retained by Two Standard Implants or 2 Mini Implants: A 3-Dimensional Finite Element Analysis. *J. Prosthet. Dent.* **2021**, *125*, 138.e1–138.e8. [CrossRef] [PubMed]
48. da Costa Valente, M.L.; Macedo, A.P.; Dos Reis, A.C. Stress Distribution Analysis of Novel Dental Mini-Implant Designs to Support Overdenture Prosthesis. *J. Oral Implantol.* **2022**, *48*, 79–83. [CrossRef]
49. Pisani, M.X.; Presotto, A.G.C.; Mesquita, M.F.; Barão, V.A.R.; Kemmoku, D.T.; Del Bel Cury, A.A. Biomechanical Behavior of 2-Implant- and Single-Implant-Retained Mandibular Overdentures with Conventional or Mini Implants. *J. Prosthet. Dent.* **2018**, *120*, 421–430. [CrossRef]
50. Solberg, K.; Heinemann, F.; Pellikaan, P.; Keilig, L.; Stark, H.; Bourauel, C.; Hasan, I. Finite Element Analysis of Different Loading Conditions for Implant-Supported Overdentures Supported by Conventional or Mini Implants. *Comput. Methods Biomech. Biomed. Eng.* **2017**, *20*, 770–782. [CrossRef]
51. Mehboob, H.; Ouldyerou, A.; Ijaz, M.F. Biomechanical Investigation of Patient-Specific Porous Dental Implants: A Finite Element Study. *Appl. Sci.* **2023**, *13*, 7097. [CrossRef]
52. Schulz, A.; Klär, V.; Grobecker-Karl, T.; Karl, M. Biomechanical Rationale for a Novel Implant Design Reducing Stress on Buccal Bone. *Appl. Sci.* **2023**, *13*, 666. [CrossRef]
53. Teodorescu, C.; Preoteasa, E.; Preoteasa, C.T.; Murariu-Măgureanu, C.; Teodorescu, I.M. The Biomechanical Impact of Loss of an Implant in the Treatment with Mandibular Overdentures on Four Nonsplinted Mini Dental Implants: A Finite Element Analysis. *Materials* **2022**, *15*, 8662. [CrossRef]
54. Lung, H.; Hsu, J.-T.; Wu, A.Y.-J.; Huang, H.-L. Biomechanical Effects of Diameters of Implant Body and Implant Platform in Bone Strain around an Immediately Loaded Dental Implant with Platform Switching Concept. *Appl. Sci.* **2019**, *9*, 1998. [CrossRef]
55. Toth, A.; Hasan, I.; Bourauel, C.; Mundt, T.; Biffar, R.; Heinemann, F. The Influence of Implant Body and Thread Design of Mini Dental Implants on the Loading of Surrounding Bone: A Finite Element Analysis. *Biomed. Eng./Biomed. Tech.* **2017**, *62*, 393–405. [CrossRef]
56. Smith, A.; Hosein, Y.K.; Dunning, C.E.; Tassi, A. Fracture Resistance of Commonly Used Self-Drilling Orthodontic Mini-Implants. *Angle Orthod.* **2015**, *85*, 26–32. [CrossRef] [PubMed]
57. Sfondrini, M.F.; Gandini, P.; Alcozer, R.; Vallittu, P.K.; Scribante, A. Failure Load and Stress Analysis of Orthodontic Miniscrews with Different Transmucosal Collar Diameter. *J. Mech. Behav. Biomed. Mater.* **2018**, *87*, 132–137. [CrossRef]
58. Freitas, C.; Leite, T.M.; Lopes, H.; Gomes, M.; Cruz, S.; Magalhães, R.; Silva, A.F.; Viana, J.C.; Delgado, I. Influence of Adhesive on Optical Fiber-Based Strain Measurements on Printed Circuit Boards. *J. Mater. Sci. Mater. Electron.* **2023**, *34*, 699. [CrossRef]
59. Liu, X.; Chen, S.; Tsoi, J.K.H.; Matinlinna, J.P. Binary Titanium Alloys as Dental Implant Materials—A Review. *Regen. Biomater.* **2017**, *4*, 315–323. [CrossRef] [PubMed]
60. Sharma, A.; Waddell, J.N.; Li, K.C.; A Sharma, L.; Prior, D.J.; Duncan, W.J. Is Titanium–Zirconium Alloy a Better Alternative to Pure Titanium for Oral Implant? Composition, Mechanical Properties, and Microstructure Analysis. *Saudi Dent. J.* **2021**, *33*, 546–553. [CrossRef]
61. Medvedev, A.E.; Molotnikov, A.; Lapovok, R.; Zeller, R.; Berner, S.; Habersetzer, P.; Dalla Torre, F. Microstructure and Mechanical Properties of Ti–15Zr Alloy Used as Dental Implant Material. *J. Mech. Behav. Biomed. Mater.* **2016**, *62*, 384–398. [CrossRef] [PubMed]
62. Zhao, Q.; Ueno, T.; Wakabayashi, N. A Review in Titanium-Zirconium Binary Alloy for Use in Dental Implants: Is There an Ideal Ti-Zr Composing Ratio? *Jpn. Dent. Sci. Rev.* **2023**, *59*, 28–37. [CrossRef] [PubMed]